Research Update: Enhancement of figure of merit for energy-harvesters based on free-standing epitaxial $Pb(Zr_{0.52}Ti_{0.48})_{0.99}Nb_{0.01}O_3$ thin-film cantilevers

Minh D. Nguyen, Evert Houwman, Matthijn Dekkers, Darrell Schlom, and Guus Rijnders

Citation: APL Materials **5**, 074201 (2017); doi: 10.1063/1.4978273
View online: http://dx.doi.org/10.1063/1.4978273
View Table of Contents: http://aip.scitation.org/toc/apm/5/7
Published by the American Institute of Physics

Research Update: Enhancement of figure of merit for energy-harvesters based on free-standing epitaxial $Pb(Zr_{0.52}Ti_{0.48})_{0.99}Nb_{0.01}O_3$ thin-film cantilevers

Minh D. Nguyen,[1,2,3,a] Evert Houwman,[1] Matthijn Dekkers,[2] Darrell Schlom,[4] and Guus Rijnders[1]

[1]*MESA+ Institute for Nanotechnology, University of Twente, P.O. Box 217, 7500AE Enschede, The Netherlands*
[2]*Solmates B.V., Drienerlolaan 5, 7522NB Enschede, The Netherlands*
[3]*International Training Institute for Materials Science (ITIMS), Hanoi University of Science and Technology, No. 1 Dai Co Viet Road, Hanoi 10000, Vietnam*
[4]*Department of Materials Science and Engineering, Cornell University, Ithaca, New York 14853, USA*

(Received 22 January 2017; accepted 24 February 2017; published online 9 March 2017)

All-oxide free-standing cantilevers were fabricated with epitaxial (001)-oriented $Pb(Zr_{0.52}Ti_{0.48})O_3$ (PZT) and $Pb(Zr_{0.52}Ti_{0.48})_{0.99}Nb_{0.01}O_3$ (PNZT) as piezoelectric layers and $SrRuO_3$ electrodes. The ferroelectric and piezoelectric hysteresis loops were measured. From the zero-bias values, the figure-of-merits (*FOMs*) for piezoelectric energy harvesting systems were calculated. For the PNZT cantilever, an extremely large value *FOM* = 55 GPa was obtained. This very high value is due to the large shifts of the hysteresis loops such that the zero-bias piezoelectric coefficient e_{31f} is maximum and the zero-bias dielectric constant is strongly reduced compared to the value in the undoped PZT device. The results show that by engineering the self-bias field the energy-harvesting properties of piezoelectric systems can be increased significantly. [http://dx.doi.org/10.1063/1.4978273]

Energy harvesting is the process of converting available ambient energy into usable electrical energy through the use of a particular material or transduction mechanism. Some of the common materials used are those with photovoltaic coupling to convert solar energy to electric energy, thermoelectric coupling to convert temperature gradients into electrical energy, and electromechanical coupling to convert mechanical vibration energy into electrical energy.[1] Piezoelectric vibration harvesting as one of the ways to realize electromechanical coupling is mainly attractive because of the simplicity of piezoelectric transduction and the relative ease of implementation of piezoelectric systems into a wide variety of applications as compared to electrostatic or electromagnetic methods.[2–5] A high piezoelectric coefficient $e_{31,f}$ value is required when a piezoelectric film has to be chosen for actuation application since the output force of a device is proportional to the piezoelectric coefficient. Therefore, high performance piezoelectric films are well suited for applications where large forces are to be produced. For energy transformation applications as in harvesters or sensors, the power efficiency of the device has to be considered as well. A benchmark for such applications is a figure of merit (*FOM*),[6]

$$FOM = \frac{e_{31f}^2}{\varepsilon_{rf}\varepsilon_0}, \tag{1}$$

which is a combination of material properties. In energy harvesting applications, e_{31f} and the relative dielectric constant of the piezoelectric film, ε_{rf}, have to be taken at zero electric field. ε_0 is the

[a]E-mail: d.m.nguyen@utwente.nl

dielectric constant of free space. Obviously to maximize the *FOM* one strives to increase e_{31f} and decrease ε_{rf}.

PZT is the most used and best developed material for many applications of piezoelectric devices. More recently much attention has been paid to alternative materials, like $0.67Pb(Mg_{1/3}Nb_{2/3})O_3$-$0.33PbTiO_3$ (PMN-PT), which (in bulk) show much larger piezoelectric effects. The highest energy-harvesting *FOM* so far, 48 GPa, was reported for an epitaxial PMN-PT thin film grown on $SrRuO_3$ (100 nm)/$SrTiO_3$ (13 nm)/Si wafers from which freestanding cantilevers were made by removal of the Si substrate.[7] The top electrode was 60-nm-thick Pt. The large *FOM* was partly due to the large e_{31f} value, but also to a large extent caused by a large field shift of the hysteresis loop of the relative dielectric constant, reducing the zero-field value significantly. However, the zero-field relative dielectric constant of this device is still fairly large. Further high quality PMN-PT thin films are not easy to grow.

In the present study, we choose for the active layer the well-studied and developed $Pb(Zr_{0.52}Ti_{0.48})O_3$ (PZT) as an active thin film material. High quality, dense, (001)-oriented, epitaxial films of PZT can be grown routinely on $SrTiO_3$ buffered Si substrates. In addition, we use $Pb(Zr_{0.52}Ti_{0.48})_{0.99}Nb_{0.01}O_3$ (1.0 wt. % Nb-doped PZT, labeled as PNZT) thin films. The Nb-doping causes a significant shift of the $e_{31f} - E$ and $\varepsilon_{rf} - E$ hysteresis loops of the PNZT-based device as compared to those of the PZT-based devices, maximizing the zero-field e_{31f} value and reducing the zero-field ε_{rf} value significantly (E is the applied electric field across the piezoelectric capacitor structure). The high obtained e_{31f} value of the PNZT film is ascribed to the high density and good crystalline quality of the films. The dielectric constant of PNZT is significantly lower than that of PMN-PT. These factors contribute to an extremely large zero-field *FOM* = 55 GPa value for the cantilever of the PNZT layer, which is the largest value reported so far. It is shown that one should be cautious using material parameter values obtained from other film stack configurations than used in the actual device. It is observed that film parameters change (deteriorate) when the substrate is removed. Hence for a fair comparison of film parameters and device performances, one should compare values obtained from similar device structures.

In this study, PZT and PNZT thin films were deposited onto SRO/$SrTiO_3$/Si substrates using a pulsed laser deposition (PLD) method.[8] The 13-nm-thick epitaxial $SrTiO_3$ (STO) buffer layer was grown by reactive molecular-beam epitaxy on Si substrates and acts as a seed layer for highly (001) oriented growth of the subsequent perovskite layers.[9] The thicknesses of the PZT and PNZT films are about 300 nm, while the top and bottom SRO electrodes are 60 nm. Details of the deposition procedure and the microfabrication process of the free-standing PZT and PNZT cantilevers with dimensions 30×75 μm are given in the supplementary material. The crystalline structure of the thin films was investigated with X-ray diffraction employing θ–2θ, rocking curves, and azimuthal ϕ-scans, using a Bruker D-8 Advance. Polarization hysteresis loops were measured with an aixACCT TF-2000 Analyzer using a triangular *ac* electric field with a frequency of 1 kHz and a maximum amplitude of 200 kV/cm. Capacitance-voltage ($C - V$) curves were determined with a Keithley4200 Semiconductor characterization system. The $C - V$ curves were measured using a slowly sweeping *dc*-electric field of 200 kV/cm amplitude with on top a 1 kHz *ac*-electric field of 4 kV/cm. The dielectric constants were calculated from the measured capacitance values. The transverse-piezoelectric coefficient (e_{31f}) is defined as the derivative of the induced in-plane stress σ_1 due to a change in the applied electrical field E_3 across the film under constant strain conditions, $e_{31}(E_3) = -(d\sigma_1/dE_3)_S$; hence it may depend on the bias point. $e_{31f} - E$ hysteresis loops were measured by applying a V_{ac} voltage excitation (33 kV/cm peak-peak amplitude, 8 kHz) to the cantilever, stepwise scanning the *dc* applied bias field between ±200 kV/cm, while measuring the tip displacement amplitude $\delta_{T,ac}$, using a lock-in measurement scheme in combination with the scanning laser Doppler vibrometer (LDV). The e_{31f} value is then extracted from the *ac* tip deflection amplitude (see supplementary material).

The crystalline structure of the PNZT thin films was investigated using X-ray diffraction. The θ–2θ scans shown in Fig. 1(a) indicate that both PZT and PNZT grow with (001) orientation without any signature of other orientations and spurious phases. The full-widths at half-maximum intensity (FWHM) of the (002) rocking curves of both the PZT and the PNZT layers are about 0.45° (Fig. 1(b)), reflecting the high orientational coherence of the films. The in-plane epitaxial relationships between the film and substrate were determined from ϕ-scans (azimuthal scans) with a tilting angle $\psi = 45°$.

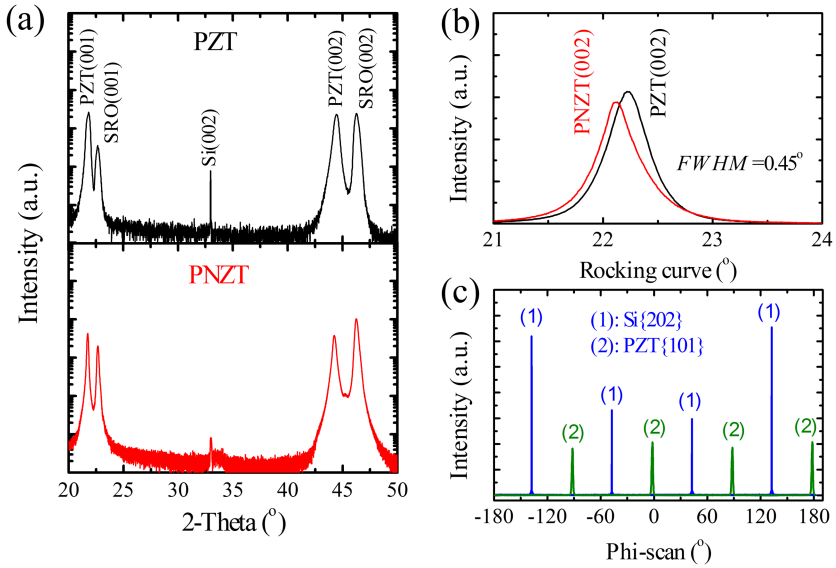

FIG. 1. (a) XRD patterns, (b) rocking curves, and (c) phi-scan of the PZT and PNZT thin films grown on SRO/STO/Si substrate.

The reflections at $\phi = -90°$, 0°, +90°, and +180° arise from the (001)-oriented PZT layer (Fig. 1(c)). The fourfold symmetry observed for the PZT films corresponds to a 45° in-plane rotated cube-on-cube epitaxy with respect to the Si substrate. From this one can deduce the following crystallographic relations between the various films and the substrate: PZT[001]//SRO[001]//STO[001]//Si[001] (out-of-plane) and PZT[100]//SRO[100]//STO[100]//Si[110] (in-plane). All indices are for a pseudocubic lattice. The same relations were obtained for the PNZT device layers.

The polarization hysteresis loops of PZT and PNZT based cantilevers films are shown in the inset of Fig. 2(a). It demonstrates that the cantilevers can be biased up to at least ±200 kV/cm without mechanical failure of the cantilever under the large curvature changes induced by these large applied fields. The *P*-*E* loop of the PNZT device shows a very large shift (self-bias field $E_{sb} = 56.2$ kV/cm) in the positive applied field direction. A positive voltage on the top electrode with respect to the bottom electrode corresponds to an externally applied field directed top-to-bottom in the piezoelectric film, while the internal built-in field causing the self-bias is directed bottom-to-top. On the other hand, the hysteresis loop of the undoped PZT shows only a small shift ($E_{sb} = -5.0$ kV/cm). As shown in the inset of Fig. 2(b), the dielectric constant versus applied field ($\varepsilon_{rf} - E$) of the PNZT device exhibits

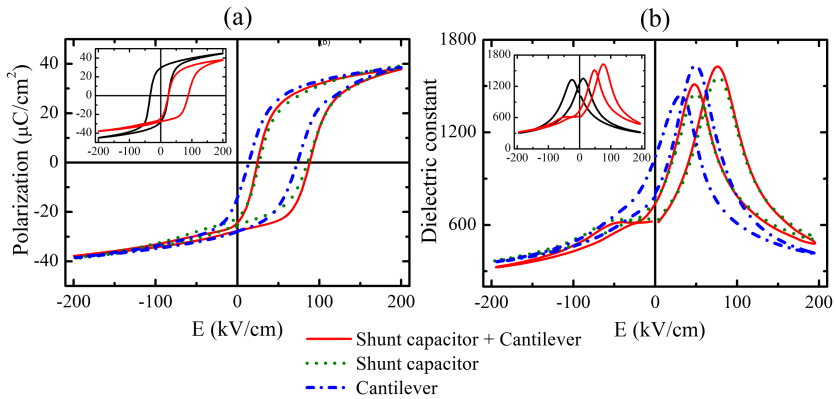

FIG. 2. (a) $P - E$ and (b) $\varepsilon_{r,f} - E$ hysteresis loops of PZT and PNZT cantilevers. The insets show the loops of the PZT and PNZT cantilever devices with a large shunt capacitor. The main figures show the loops of the PNZT device with (solid red) and without shunt (dashed blue) and the shunt capacitor alone (dotted green).

a similar shift as the *P-E* loop (The "zero-field crossing"– indicated by the red dot in the inset of Fig. 2(b)– is shifted by 59.9 kV/cm). Evidently the decrease in dielectric constant at zero electric field in the PNZT thin films caused by the self-bias will lead to an enhancement of the *FOM* for piezoelectric energy harvesting systems operating at zero applied field.

Baek *et al.* argued that the asymmetry of the top (Pt) and bottom (SRO) electrode materials played an important role in the self-bias of the polarization and permittivity hysteresis loops in their SRO/PMN-PT/Pt device.[7] Lee *et al.*[10] suggested that an asymmetry in the oxygen vacancy content was the cause of the *P-E* loop shift in their $Pb_{0.9}La_{0.1}Zr_{0.2}Ti_{0.8}O_3$ (PLZT) thin film capacitors with $La_{0.5}Sr_{0.5}CoO_3$ top and bottom electrodes. It was argued that the concentration of oxygen vacancies in and near the top electrode changes, while that at the bottom electrode basically remains unchanged for cooling down under different oxygen atmosphere pressures after deposition. Here the PZT and PNZT thin films are sandwiched symmetrically between SRO electrodes of equal thickness, which were deposited under the same conditions and cooled down in the same high oxygen pressure atmosphere. Thus one can assume that the electrodes are to a large extent symmetric in properties. Since the layer stack is the same for the PZT and PNZT devices, except for the doping of the latter, the large self-bias in our epitaxial PNZT films must be related to the Nb-doping. Although one would expect from the used pulsed laser deposition process a homogeneous Nb-doping throughout the film, the large positive self-bias suggests an asymmetric charge distribution in the film, since a homogeneous charge doping would not cause self-bias in a symmetric device. We speculate that there is a positive charge build-up in the initial PNZT growth layer at the base electrode and the PNZT film interface. In this initial growth layer, epitaxial strain is released by defect incorporation during growth, causing strain gradients and possibly a composition variation. The presence of such a strain relaxation layer was shown before to be present in the epitaxial ferroelectric thin film stacks and could explain the observed large self-bias in these capacitors.[11] The nature and cause of this charge profile and its cycling stability are subject of further study.

It is to be noted that the cantilever capacitor is shunted by a capacitor on the Si-base of the structure formed by the same layer stack as the cantilever (Fig. S2(a) of the supplementary material). The area of this shunt capacitor is approximately 15 times larger than the area of the cantilever, thus the shape and self-bias of the $P - E$ and the $\varepsilon_{rf} - E$ hysteresis loops and therefore the zero-field dielectric constant may be dominated by the clamped electrode film of the shunt capacitor. To study the effect of the shunting, we cut off the largest part of the top electrode by focused ion beam (FIB) milling (Fig. S2(b)). In this way, the shunt capacitor area was reduced to about 1/3 of the cantilever area and we can assume that the properties of the remaining structure are determined largely by those of the cantilever area.

Fig. 2(a) shows the $P - E$ loops of the cantilever and the large shunt capacitor after the FIB-cutting, together with the original loop of the cantilever with the large shunt. It is observed that the loop of the shunt capacitor has the same self-bias as the cantilever with the shunt, as expected, whereas the self-bias of the cantilever is slightly less than that of the shunt capacitor. Removing the substrate thus changes the self-bias in the film and it is seen that it also makes the loop more symmetric than that with the shunt capacitor. It has no effect on the high-field polarization values. Similar effects are observed in the $\varepsilon_{rf} - E$ loop of the cantilever with shunt and the shunt capacitor alone compared to the cantilever without shunt (Fig. 2(b)). Note the difference in zero-field ε_{rf} value for the falling branch and rising branch of the loops. These values are relevant for calculating the *FOM* value of a cantilever. One can choose either of these zero-field operation points and its associated value of ε_{rf}, by cycling to positive respectively negative high field and then return to the zero bias point. At present it is unclear what causes the plateaus in the rising and falling branches of the $\varepsilon_{rf} - E$ loop of the PNZT capacitor, but it is likely to be connected to the asymmetry of the charge distribution in the shunt part of the device layer. The plateau has completely disappeared in the loop of the cantilever without shunt. The difference in maximum dielectric constant of the rising and falling branches reflects an asymmetry in the device stack, which is present in the cantilever as well as in the shunt capacitor and is also attributed to the asymmetric charge distribution causing the self-bias in these loops. For the cantilever, $\varepsilon_{rf} = 1040$ for the falling branch and 810 for the rising branch. This is considerably more than that for the cantilever with the shunt ($\varepsilon_{rf} = 740$ and 620, respectively). This is due to the reduced self-bias (40.0 kV/cm) of the loop of the cantilever as compared to the 59.9 kV/cm of the

dielectric loop of the cantilever with shunt. These aspects demonstrate the importance of measuring the dielectric properties of the cantilever alone to determine the *FOM* and not the properties that are dominated by a shunt capacitor or of a clamped film structure (as was done in Ref. 7).

Fig. 3(a) shows a top-view scanning electron microscope image of a free-standing, unbiased SRO/PNZT/SRO/STO cantilever (30 × 75 μm). Fig. 3(b) gives a typical white-light interferometer measurement of the static bending of this cantilever under applied field. The thermal expansion difference between the STO buffer layer (*TEC*(STO) ≈ 11 ppm/K) and a symmetric SRO/PZT/SRO stack (*TEC*(PZT) ≈ 6 ppm/K) would in theory cause a downward curvature of the cantilever after release from the Si substrate. However an upward curvature is observed for both the PZT and the PNZT cantilevers. We explain the upward curvature by compressive stress release in the initial growth part of the PNZT layer, closest to the Si-substrate. During deposition, this layer is severely compressively stressed because of the cube-on-cube growth on the underlying STO/SRO layers which have significantly smaller lattice constants than the PNZT. As mentioned, we observed such a compressively strained initial growth layer before.[11] With increasing thickness this stress is relaxed by the incorporation of defects so that for film thicknesses beyond about 10–20 nm the PNZT adopts its bulk (pseudocubic) lattice parameter. When the clamping is removed on removal of the Si substrate the compressively stressed layer expands in the plane of the cantilever causing the net upward curvature. The upward bending moment due to the compressive stress release appears to be stronger than the small downward bending moment due to the thermal stress buildup between the thin STO layer and the PNZT. Fig. 3(c) gives the $e_{31f} - E$ hysteresis loops of the PZT and PNZT cantilevers (with the capacitive shunt) determined with an *ac* lock-in measurement technique (see supplementary material).

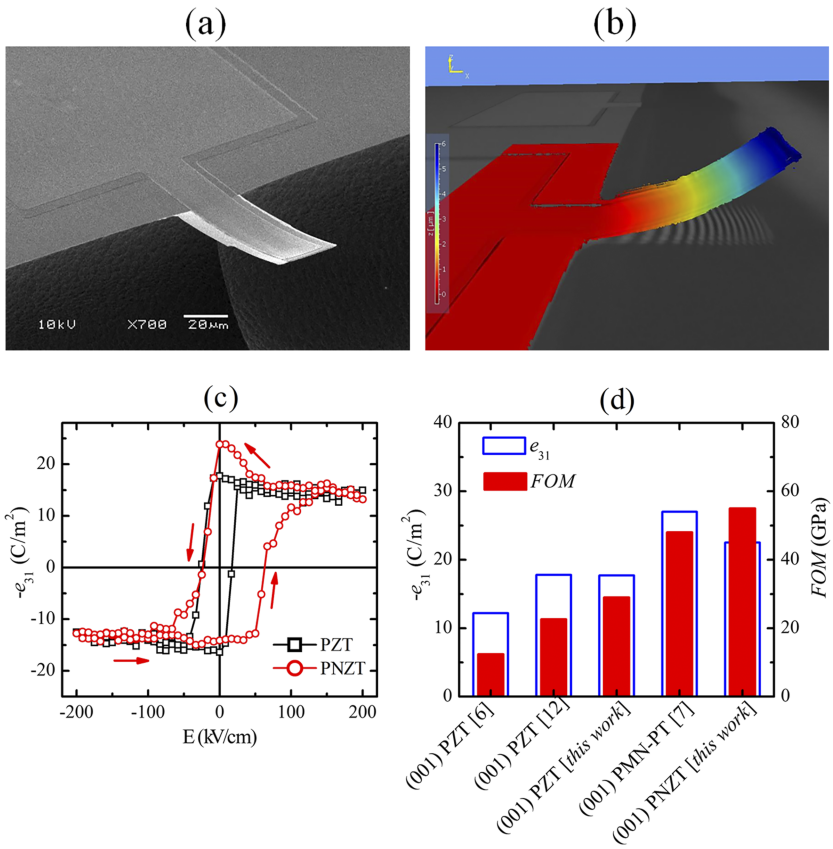

FIG. 3. (a) Top-view SEM image. (b) Static white-light interferometer measurement showing the 3D view of a free-standing PNZT cantilever (30 × 75 μm). (c) Transverse piezoelectric coefficient $e_{31f} - E$ loops of PZT and PNZT cantilevers (with shunt capacitor). (d) Comparison of values of the figure of merit (*FOM*) and the piezoelectric coefficient (e_{31f}) of the PZT and PNZT cantilevers (without shunt capacitor) of this work with other reported values: sol-gel (001) PZT52/48 on Pt buffer,[6] gradient-free sol-gel (001) PZT52/48 on Pt buffer,[12] and off-axis sputtered (001) PMN-PT on STO-buffered Si.[7]

There is hardly any difference between the loops of the cantilevers with and without the shunt capacitor, as one would expect since in both cases the $e_{31f} - E$ hysteresis loop is determined from the bending of the cantilever directly and not from charge measurements. Such a method gives a more reliable estimate of the piezoelectric constant in the cantilever than with the wafer flexure experiments in which the film stack is still clamped, because (i) e_{31f} is determined under *ac* conditions as are applicable in the operation of an energy harvesting device and (ii) the stress in the cantilever associated with the clamping is largely released (causing also the upward curvature). Both the coercive field (E_c = 45.8 kV/cm) and the self-bias (E_{sb} = 16.7 kV/cm) of the (dynamic) $e_{31f} - E$ hysteresis loop are significantly different from the values of the $P - E$ loop of the PNZT cantilever (smaller E_c = 29.4 kV/cm and larger E_{sb} = 43.6 kV/cm, respectively). The $e_{31f} - E$ loop shift of the PZT cantilever is only −4.2 kV/cm, well comparable to that of the $P - E$ loop (−5.0 kV/cm), while the coercive fields are closer, 20.8 and 28.9 kV/cm, respectively. Thus it appears that the large differences in self-bias and coercive field of the $P - E$ and the $e_{31f} - E$ loops are related to the Nb doping. However we have no more fundamental explanation for these observations yet. The loop of the PZT device (with shunt) shows a slightly increased value on the falling branch with $|e_{31f}(0)|$ = 17.7 C/m^2 and 16.4 C/m^2 on the rising branch. These values are well comparable to the best values for PZT reported in the literature,[12] suggesting that this property saturates at this value for high quality and high density thin films. The higher *FOM* of our PZT device (*FOM* = 29 GPa) compared to that of Ref. 12 is due to its significantly lower dielectric constant. The hysteresis loop of the PZT-driven cantilever is fairly symmetric, whereas that of the PNZT-driven cantilever shows a pronounced increase of $e_{31,f}$ for small positive field values in the falling branch. For higher field values, the e_{31f} values are the same as for the PZT device. We think that it is plausible to attribute the asymmetry of the curve at low fields to the assumed asymmetric charge distribution in the doped PZT, which is used to explain the self-bias in the PNZT device. Consequently one can use the enhanced zero-field piezoelectric coefficient for improved energy harvesting by pre-poling the device positively. The largest *FOM* is obtained at zero field (in the PNZT cantilever without the shunt capacitor) where $|e_{31f}(0)|$ = 22.5 C/m^2 and $\varepsilon_r(0)$ has dropped already significantly to 1040, due to the $\varepsilon_{rf} - E$ loop shift. In this situation, the zero field figure of merit of the PNZT cantilever is obtained, $FOM(0)$ = 55 GPa, which is also the maximum. The maximum $|e_{31f}|$ value is 23.2 C/m^2 on the falling branch of the loop, whereas on the rising branch it is 14.1 GPa.

Fig. 3(d) compares the $|e_{31f}(0)|$ and *FOM* values in this study with the best values of previously reported works.[6,7] Although the piezoelectric coefficient of the PNZT cantilever is slightly less than that of the PMN-PT cantilever,[7] the *FOM* value of the PNZT film is significantly larger. Here we make the annotation that for our device the $e_{31f}(0)$ and $\varepsilon_r(0)$ values, from which the *FOM* is calculated, have been determined from the same cantilever in dynamic mode, whereas in Ref. 7 these values were deduced from the static bending of a clamped thin film stack and not from a cantilever itself. As discussed above, this may cause significant differences with the values of an actual oscillating cantilever. Indeed if the $\varepsilon_r(0)$ value of the PNZT shunt capacitor is used, a *FOM* value as high as 82 GPa is obtained. The large *FOM* of our PNZT device is caused by the significantly lower relative dielectric permittivity than that of the PMN-PT device (maximum values in the falling branches are, respectively, 1518 and about 2650 for the PNZT and PMN-PT cantilevers, respectively), whereas the reduction of the zero-field relative dielectric permittivity due to loop-shift ($\varepsilon_{rf,max}/\varepsilon_{rf}(0) \approx 1.5$) is approximately the same for the PNZT and PMN-PT devices. The significantly lower $\varepsilon_r(0)$ of the PNZT device overcompensates the slightly smaller $e_{31f}(0)$ compared to the values of the PMN-PT device, giving rise to the larger *FOM* value.

In summary, (001)-epitaxial PZT and Nb-doped PZT (PNZT) thin films were fabricated on STO buffered Si substrates with top and bottom SRO electrodes. Freestanding all-oxide cantilevers were obtained by selectively etching the Si substrate. It is shown that by the combination of a relatively low dielectric constant of PNZT with a large shift of the ferroelectric loop, caused by the Nb-doping of the PZT layer, a very large figure of merit for energy-harvesting applications can be obtained. The enhanced piezoelectric coefficient at zero field is attained by choosing the right branch of the piezoelectric hysteresis loop of the PNZT device. The obtained *FOM* value (55 GPa) is significantly larger than the best result reported so far obtained with freestanding PMN-PT cantilevers. The piezoelectric constant of the undoped PZT is comparable to that of the

best PZT films reported in the literature, but the figure of merit is increased because of a lower dielectric constant. Because the undoped PZT films do not show loop shifts, the figure-of-merit is much less than that of the PNZT devices. It is also shown that one should be very cautious using material parameters determined from clamped film structures to calculate the *FOM* of a piezoelectric stack released from the substrate. These results demonstrate that by optimizing the properties of PZT thin films by using improved buffer layers (STO-buffered Si) and doping in order to induce self-bias in the hysteresis loops, there is ample room to increase the energy-harvesting properties of piezoelectric systems significantly without the need to change the active material.

See supplementary material for the microfabrication process for free-standing PNZT cantilevers; top-view microscope image of a free-standing PNZT cantilever (30×75 μm); transverse piezoelectric coefficient (e_{31f}) calculation.

We acknowledge the financial support provided by the Dutch GO EFRO-funded "I2I" program (Innovation 2 Industrialization for advanced micro- and nanosystems) and by NanoNextNL, a micro and nanotechnology consortium of the Government of the Netherlands and 130 partners.

[1] S. R. Anton, "Multifunctional piezoelectric energy harvesting concepts," Ph.D. thesis, Virginia Polytechnic Institute and State University, Virginia, USA, 2011.
[2] S. J. Roundy, "Energy scavenging for wireless sensor nodes with a focus on vibration to electricity conversion," Ph.D. thesis, The University of California, Berkeley, USA, 2003.
[3] S. Roundy, J. Intell. Mater. Syst. Struct. **16**, 809 (2005).
[4] Y. Zhao, Q. Liao, G. Zhang, Z. Zhang, Q. Liang, X. Liao, and Y. Zhang, Nano Energy **11**, 719 (2015).
[5] G. Zhang, Q. Liao, M. Ma, Z. Zhang, H. Si, S. Liu, X. Zheng, Y. Ding, and Y. Zhang, Nano Energy **30**, 180 (2016).
[6] S. Trolier-McKinstry and P. Muralt, J. Electroceram. **12**, 7 (2004).
[7] S. H. Baek, J. Park, D. M. Kim, V. A. Aksyuk, R. R. Das, S. D. Bu, D. A. Felker, J. Lettieri, V. Vaithyanathan, S. S. N. Bharadwaja, N. Bassiri-Gharb, Y. B. Chen, H. P. Sun, C. M. Folkman, H. W. Jang, D. J. Kreft, S. K. Streiffer, R. Ramesh, X. Q. Pan, S. Trolier-McKinstry, D. G. Schlom, M. S. Rzchowski, R. H. Blick, and C. B. Eom, Science **334**, 958 (2011).
[8] M. D. Nguyen, E. Houwman, M. Dekkers, H. N. Vu, and G. Rijnders, Sci. Adv. Mater. **6**, 243 (2014).
[9] M. P. Warusawithana, C. Cen, C. R. Sleasman, J. C. Woicik, Y. Li, L. F. Kourkoutis, J. A. Klug, H. Li, P. Ryan, L. P. Wang, M. Bedzyk, D. A. Muller, L. Q. Chen, J. Levy, and D. G. Schlom, Science **324**, 367 (2009).
[10] J. Lee, R. Ramesh, V. G. Keramidas, W. L. Warren, G. E. Pike, J. T. Evans, Jr., Appl. Phys. Lett. **66**, 1337 (1995).
[11] M. Boota, E. P. Houwman, M. Dekkers, M. Nguyen, and G. Rijnders, Appl. Phys. Lett. **104**, 182909 (2014).
[12] J. F. Shepard, Jr., P. J. Moses, and S. Trolier-McKinstry, Sens. Actuators A **71**, 133 (1998).